We are IntechOpen, the world's leading publisher of Open Access books Built by scientists, for scientists

6,900
Open access books available

185,000
International authors and editors

200M
Downloads

Our authors are among the

154
Countries delivered to

TOP 1%
most cited scientists

12.2%
Contributors from top 500 universities



WEB OF SCIENCE™

Selection of our books indexed in the Book Citation Index in Web of Science™ Core Collection (BKCI)

Interested in publishing with us?
Contact book.department@intechopen.com

Numbers displayed above are based on latest data collected.
For more information visit www.intechopen.com



3

Microsystem Technologies for Biomedical Applications

Francisco Perdigones, José Miguel Moreno,
Antonio Luque, Carmen Aracil and José Manuel Quero
University of Seville
Spain

1. Introduction

Microsystems, also often known as microelectromechanical systems (MEMS), are miniaturized devices fabricated using techniques called "micromachining", and that are common in different application areas, such as automotive, consumer electronics, industrial measurements, and recently biomedical too Dean & Luque (2009). The typical definition states that a microsystem is any device which has at least one feature size in the order of micrometers (1:1000 of a mm).

Historically, silicon has been used as the material of choice for fabricating microsystems, due to the processing equipment which was already available in microelectronics foundries, and the thorough understanding of the properties that the impressive development of electronics in the 1950s and 60s made possible. Another advantage derived from microelectronics is the low cost associated when fabricating devices at very large production volume. It was then natural to try to integrate other devices with the microelectronic chips, and so the first microsystems were born. Initially, the market was driven by automotive applications, and accelerometers for stability control and airbag deployment were one of the first commercial successes of microsystems technology. Other typical examples from this age are pressure sensors and inkjet printer nozzles. Since then, the global MEMS market has not ceased to grow, and their applications are more diverse now. It is expected that by 2010 more than 8000 million MEMS devices will be sold yearly *Status of the MEMS industry* (2008).

As explained before, due to the importance of the microelectronics foundries, silicon is nowadays a widely available material, with a relatively low cost. Its mechanical and electrical properties have been very well known for decades, a fact which still makes it an ideal choice for many microsystems. Silicon is nearly as strong as steel, but with a much lower fracture toughness Petersen (1982). It is usually sold in circular wafers of varying diameters, from 100 to 500 mm. In microsystems, the final devices are sometimes built by removing part of the material in the substrate, in a process called bulk micromachining, while in other occasions, thin films are deposited on top of the wafer and then parts of them are etched away to form the device, which is known as surface micromachining Kovacs et al. (1998). The actual micromachining of silicon is performed using etchants, which can be liquid (wet etching) or in gas or plasma form (dry etching). Both types can etch the silicon isotropically or anisotropically, depending on the etchant composition and operating parameters. Other materials are commonly present in silicon-based microsystems, most of which also derive from silicon, such as polycrystalline silicon, silicon dioxide, or silicon nitride. Thin or thick

films of other materials can be deposited on top of the substrate using chemical vapor deposition (CVD), sputtering, thermal evaporation, or spin coating, among other techniques. All the mentioned process are complemented by photolithography, by means of which a particular area of the wafer where to etch or deposit a material can be selected. This is done using a photosensitive resist which is exposed to light (usually ultraviolet) through a mask with opaque and transparent areas. The resist is then developed and the exposed areas are removed (if the photoresist is positive). The remaining photoresist protects the wafer and avoid that area to be etched away, or a material to be deposited on top of it.

Silicon has been used successfully to fabricate devices such as microfluidic control valves, blood micropumps and microneedles for drug delivery through the skin Henry et al. (1998), but other materials are of more importance for biomedical applications. These materials are usually polymers, which offer the advantage of being cheap and fast to process, especially for small-scale production. Many of the polymers used are biocompatible.

Two of the most common used polymers are PMMA (poly-methyl-metacrylate) and PDMS (poly-dimethyl-siloxane). PMMA is available in solid form, and thermal casting or molding are used to shape it Huang & Fu (2007). PDMS is available as two liquid products (prepolymer and curing agent), which should be mixed together, poured over a mold, and cured at moderately high temperatures. Then it becomes solid and can be demolded. This process has been widely adopted by the microfluidics and biomedical communities since it was developed in 2000 Duffy et al. (1998). Another material used in rapid prototyping is the negative photoresist called SU-8. Examples of actual devices built using PDMS and SU-8 will be showcased below.

The measurement of substances in the blood was one of the first biomedical applications of MEMS devices. Nowadays, personal glucometers are inexpensive, and some of them are starting to include an insulin pump, also built with MEMS technology, which is able to deliver insulin to the patient when the measured glucose level is too high.

One of the most important goals of the research in BioMEMS is the fabrication of a lab-on-chip (LOC) device, where all the needed components to perform extraction, movement, control, processing, analysis, etc. of biological fluids are present. This LOC device would be a truly miniaturized laboratory, which would fulfill many of today's needs in portable medicine.

To accomplish a task like building a LOC, many smaller parts must be considered. In the rest of the sections of this chapter, these parts will be discussed. Section 2 will discuss in detail the fabrication processes for the materials described above, which are the most commonly used now. In Section 3, the issue of power supply will be considered, and some solutions to integrate the microfluidic power in the microsystem will be presented. Section 4 will deal with control and regulation of biological fluids inside the chip. In Section 5, the integration of the different components will be discussed, giving some examples of actual devices, and finally in Section 6, some conclusions will be remarked.

2. Fabrication processes for biocompatible materials

2.1 Introduction

In this section the basis of fabrication processes using the most commonly biocompatible polymers used in MEMS are reported. These materials are Glycidyl-ether-bisphenol-A novolac (SU-8) Lorenz et al. (1997) and polydimethilsiloxane (PDMS) McDonald & Whitesides (2002).

Regarding SU-8 fabrication processes, the typical fabrication process and multilayer technique Mata et al. (2006) are presented in this introduction. Then, in section 2.3 a new process to

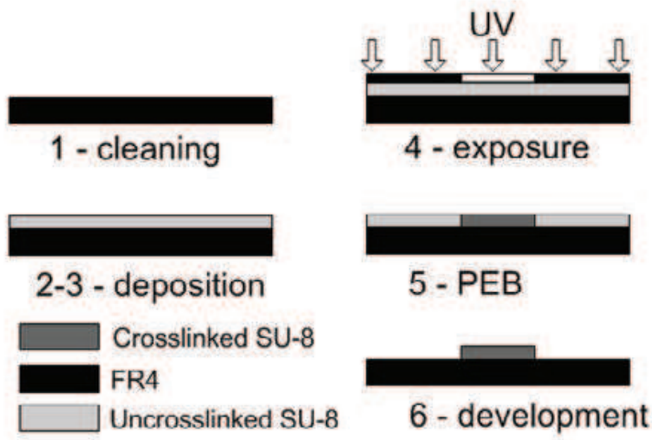


Fig. 1. Typical SU-8 process

transfer SU-8 membranes are commented in order to achieve closed structures. The PDMS material is also presented in this introduction together with the facilities used to process both materials. Neither applications nor functionality of the fabricated devices are presented in this section, only the materials, equipment and processes are reported.
SU-8 is a negative epoxy photoresist widely used in MEMS fabrication, above all in microfluidics and biotechnology due to its interesting properties such as biocompatibility, good chemical and mechanical resistance, and transparency. The typical fabrication process of SU-8 Lorenz et al. (1997) has the following steps as is shown in Fig. 1.

1. Cleaning: The substrate is cleaned using the appropriated substances.
2. Deposition: Deposition by spin coating. The equipment in this step is a spin coater thanks to the thickness of deposited layer can be controlled.
3. Softbake: Softbake in a hot plate, in order to remove the solvent and solidified the deposited layer.
4. Exposure: The SU-8 layer is exposed to ultraviolet UV light using an appropriate mask. The exposed SU-8 will crosslink whereas not exposed SU-8 will be removed. In this step a mask-aligner is necessary in order to align the different masks and expose.
5. Post exposure bake (PEB): The layer is baked using a hot plate in order to crosslink the exposed SU-8.
6. Development: The uncrosslinked SU-8 is developed by immersion and agitation using a developer, e.g., PGMEA.

Times, exposing doses and temperatures are proposed by the SU-8 manufacturer, e.g., MicroChem Corporation or Gersteltec Engineering Solutions.
The SU-8 multilayer technique is used to achieve different thickness in the fabricated structure. This procedure of fabrication consists of performing the previous steps 2 to 5 and them these steps are carried out as many times as additional different thicknesses are required. The final step is a development of the whole structure. In Fig. 2 a multilayer process (two layers) is depicted.
Polydimethylsiloxane (PDMS) is an elastomer material with Low Young modulus. In this respect, PDMS is more flexible material than SU-8. PDMS is also widely used in microfluidic

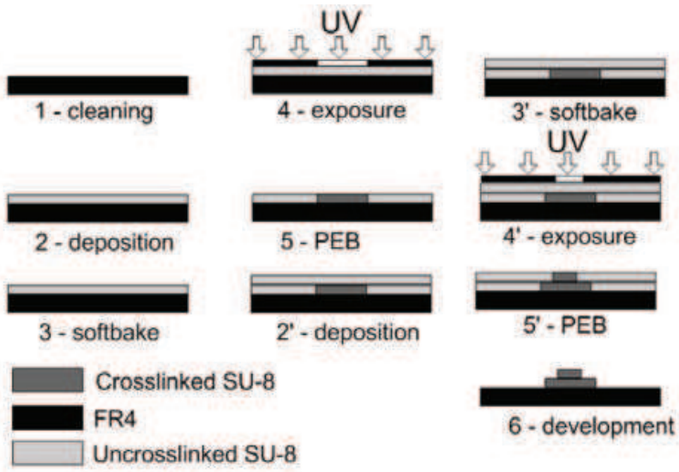


Fig. 2. Multilayer SU-8 process

circuits and biotechnology as base material. It is composed by a prepolymer and a curing agent that must be mixed in order to obtain the PDMS. Depending on the ratio of both substances the PDMS will require a certain time of curing for a fixed temperature. The equipment necessary to process PDMS includes a vacuum chamber to remove the bubbles that appear during mixing and an oven to cure the PDMS. The fabrication of PDMS device is preceded by molds fabrication. These molds are necessary to define the PDMS structure as it will be explained.

2.2 PDMS fabrication processes

The fabrication using PDMS elastomer is based on soft lithography McDonald & Whitesides (2002). The procedure starts with the fabrication of molds. There are several techniques to fabricate these molds, among others, photolithography or micromachining. The substrate widely used for photolithography is silicon, and the material to define the structures is SU-8. The molds are fabricated using the typical process of SU-8 or using more complex techniques as multilayer fabrication. The low adherence of PDMS to SU8 and silicon facilitates the demolding process. We propose Flame Retadant 4 (FR4) of Printed Circuit Board (PCB) as substrate due to its low cost and good adherence with SU-8, Perdigones, Moreno, Luque & Quero (2010). However this material presents more roughness than silicon or pyrex but no problems have been observed due to this issue. A mold fabricated performing the typical process with FR4 as substrate and SU-8 can be seen as an example in Fig. 3. As it is explained later, the PDMS will be poured over it, achieving the negative pattern of the mold.

Once the molds have been produced, a mixture of prepolymer and curing agent is performed with a commonly used ratio in weight percent of 10:1. This mixture is performed by agitation using a stirring bar, and then is degassed in order to remove the bubbles that appear during mixing. Once the mixture has been degassed, it is poured over the mold and put into an oven at 65 °C during 1 h approximately until PDMS is crosslinked and solidified. Finally, the PDMS is peeled off the mold. Using this method only opened structures or microchannels can be fabricated.

There are several techniques of PDMS to PDMS bonding in order to complete the fabrication and achieve the closed structures Eddings et al. (2008). Among these techniques, Partial

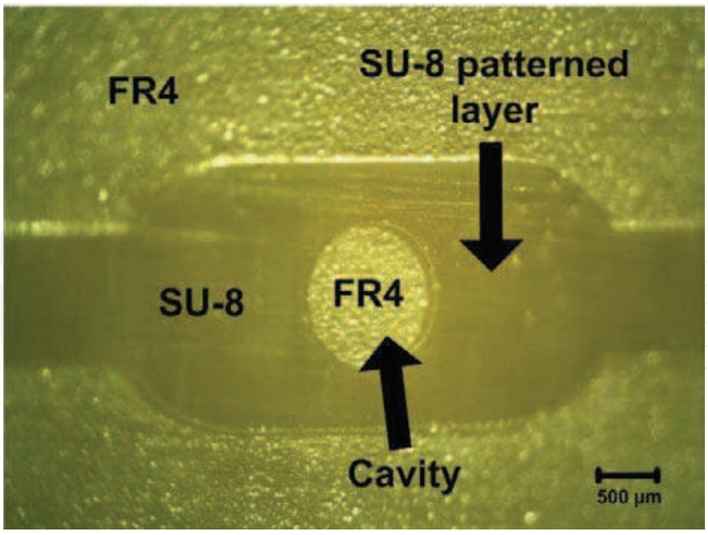


Fig. 3. Fabricated mold using FR4 as substrate and SU-8 to define the structure. The SU-8 patterned layer defines a microchannel with an internal column due to the central cavity.

Curing, Uncured PDMS adhesive and Varing Curing Ratio are the most interesting ones due to their high average bond strengths. In literature, authors propose different temperatures, baking times and ratios to perform the bonding using these techniques. In this respect, our group uses a combination of Partial Curing and Varing Curing Ratio with successful results in multilayer fabrication. We use a ratio 20:1 and 10:1 alternatively, i.e., 20:1 for the first layer, 10:1 for the second one, for the third layer 20:1, etc. The baking times can be selected in a range of 30-45 min for 10:1 ratio, and 50-60 min for 20:1 ratio, at 65 °C in an oven. Finally, the bonding is performed at 65 °C during 2 h in the oven. In Fig. 4, the PDMS part of an extractor of liquid for submicroliter range Perdigones, Luque & Quero (2010b) can be seen.
In order to fabricate the PDMS structure shown in Fig. 4 only one mold is necessary. The procedure of fabrication is very simple, where two PDMS pieces are bonded. This process can be seen in Fig. 5 and it starts with the fabrication of the mold using the SU-8 typical procedure. Once the mold has been done, a PDMS with a ratio of 10:1 is poured over it (layer 1), step (a),

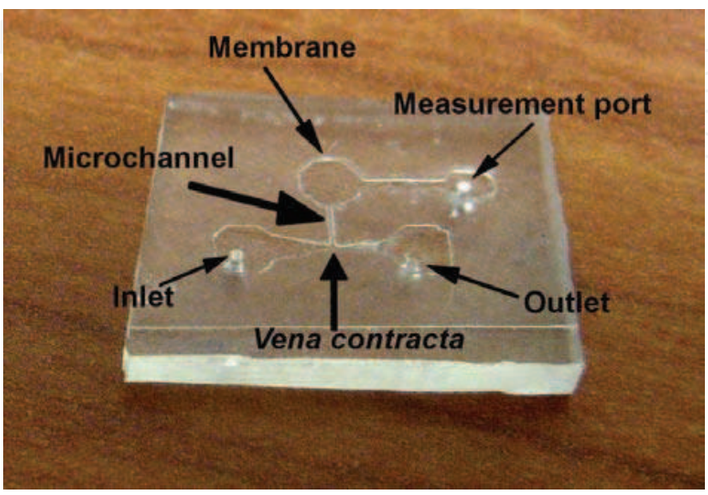


Fig. 4. PDMS extractor of liquid for submicroliter range.

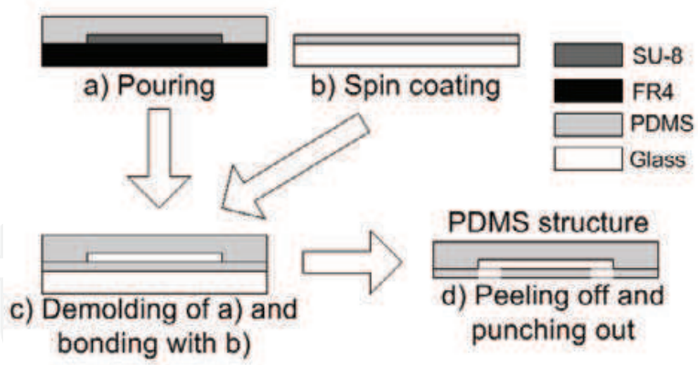


Fig. 5. Fabrication process for the structure in Fig. 4

and other mixture of 20:1 is spin coated over a glass substrate (layer 2), step (b). The layers are put into an oven at 65 °C during 45 min for the first one and 1 h for the second one. Then, the layer 1 is demolded and put into contact to layer 2, (step c), as can be seen in Fig. 5 and the bonding is performed in an oven at 65 °C during 2 h. Once the bonding has been performed, the final structure is peeled off the glass substrate and the layer 2 is punched out.

A more complex PDMS three dimensional structure with three different layers and fabricated using the presented process is shown in Fig. 6. This is a cross section of a PDMS flow regulator with positive gain as will commented in section 4.

The process to fabricate the structure in Fig. 6 requires two molds and is shown in Fig. 7. The first one (mold 1) is made using the typical process and the second one (mold 2) using the multilayer technique. The procedure starts performing three mixtures with a ratio 10:1 for the intermediate layer (layer 2) and 20:1 for the rest. Once the mixtures have been degassed, the mixture 10:1 is spin coated over the mold 1 in order to achieve a structure (layer 2) with a membrane on top (step a). Next, one of 20:1 mixture is poured over the mold 2 (step b) defining the layer 1, and the other is spin coated over a glass substrate (step c) defining the layer 3. All layers are put into an oven at 65 °C during 30 min for layer 2 and 1 h for the rest. Once the PDMS layers are partially curing, layer 1 is demolded and put into contact with layer 2 as can be seen in step d. Both layers are put into an oven at 65 °C during 5 min in order to achieve a initial bonding. This bonding is necessary to demold layer 2 without breaks that might appear due to its low thickness. Once this initial bonding is performed, the structure is

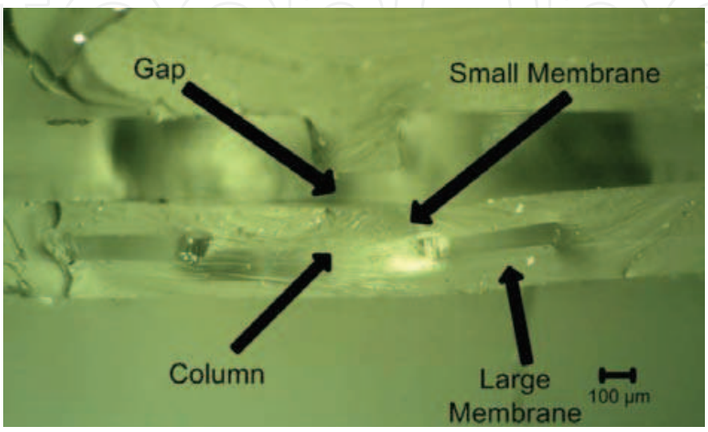


Fig. 6. Three dimensional PDMS structure with three layers

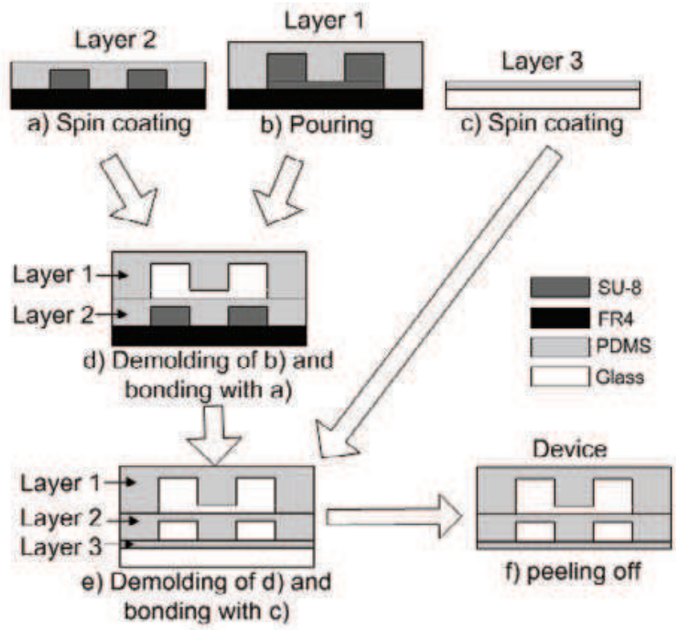


Fig. 7. Fabrication process for the structure in Fig. 6

demolded from mold 1, and put into contact with layer 3 as can be seen in step e. Next, these three layers are bonding at room temperature during 24 h because the air in the cavities could expand and lead the separation between layer 2 and 3. After this step, the final structure is put in a hot plate at 50 °C during 5 min to ensure a good bonding and then the device is peeled off the glass substrate.

2.3 SU-8 closed structures

A special effort is associated to processes which achieve 3D structures to fabricate microchannels and microreservoirs, taking into account that SU-8 typical process is focused for the fabrication of open structures.

Different ways to achieve SU-8 closed structures have been reported but mainly we can find two trends. The first approach employs sacrificial layers, where uncrosslinked SU-8 is used as base to obtain upper layers and afterwards it is removed. A microchannel fabricated by this method is shown in Fig.8. The significant disadvantages of this approach are the limitation of the design of structures with an aperture to strip off the uncrosslinked SU-8, and an excessive development time for the required multilayer deposition Chung & Allen (2005). However, in recent years there is an evolution in various aspects of this approach improving the mask-process Guerin et al. (1997), embedding the masks Haefliger & Boisen (2006), and controlling the exposure, Chuang et al. (2003).

The second trend widely used, consists in sealing the SU-8 structure by means of transferring SU-8 layers. In this way, the use of removable films to transfer SU-8 layers obtaining monolithic devices by lamination has been broadly reported. Many different materials are used as removable layer, among others, PDMS Patel et al. (2008), PET Abgrall et al. (2008), kapton Ezkerra et al. (2007). Besides from using different materials, there are plenty of flow processes based in the transfer of the SU-8 layers as well. An important requirement in the development of processes is the compatibility with previous processes to be able to improve the complexity and integration with other devices.

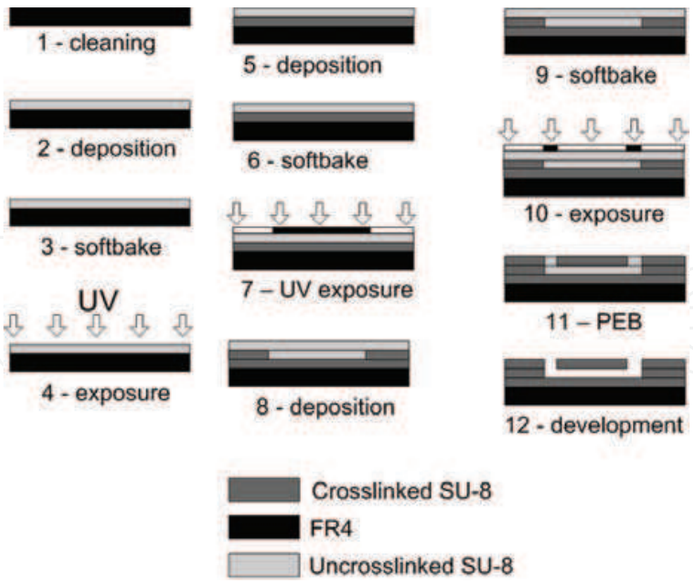


Fig. 8. Flow of fabrication process of a sacrificial layer process.

A particular example of this approach is the transferring process has been named BETTS Aracil, Perdigones, Moreno & Quero (2010) (Bonding, UV Exposing and Transferring Technique in SU-8). The key step of this process is the use of the layer substrate not only to transfer the SU-8 layer, but also to act as a mask to pattern the SU-8 layer and to allow peeling off the transferred film easily. Therefore, bonding, UV exposing and transferring processes are carried out in a single step. The process flow of BETTS can be seen in Fig. 9. The transfer process can be achieved over different kind of substrates, like glass, silicon, SU-8 or FR4, what extends the number of applications that can use of it. The thickness of the transferred layer is variable according to the application. Its value is very closed linked to the height of the microchannel. The shallowest microchannel fabricated corresponds to 40μm, for a thickness of the transferred layer of 5μm. The compatibility with others fabrication processes allows the integration with other electronic devices wire bonded to the substrate. 3D structures are easily manufactured by means of the repetition of the flow of process. An example of 3D multichannel network is shown in Fig. 10.

3. Autonomous microdevices

3.1 Pressure chambers

Nowadays, an important challenge still to be overcome in the field of Lab on Chip devices is the improvement of portability and fluid flow generation. Although there is a wide range of methods to develop fluid flow in microfluidic devices such as electroosmotic flow, electrokinetic pumps or by centrifugal force or capillary action, Laser & Santiago (2004); Lim et al. (2010), on-chip pumping is in general externally generated by traditional macroscale syringe or vacuum pumps. This limitation makes LOC devices encapsulation and portability a very difficult task when developing miniaturized autonomous microfluidic systems. Moreover, MEMS packaging results more expensive compared to the microsystem itself when considering vacuum or pressure sealing, being indispensable to find simple and low cost encapsulation methods fully compatible and easy to integrate with former fabrication processes and materials.

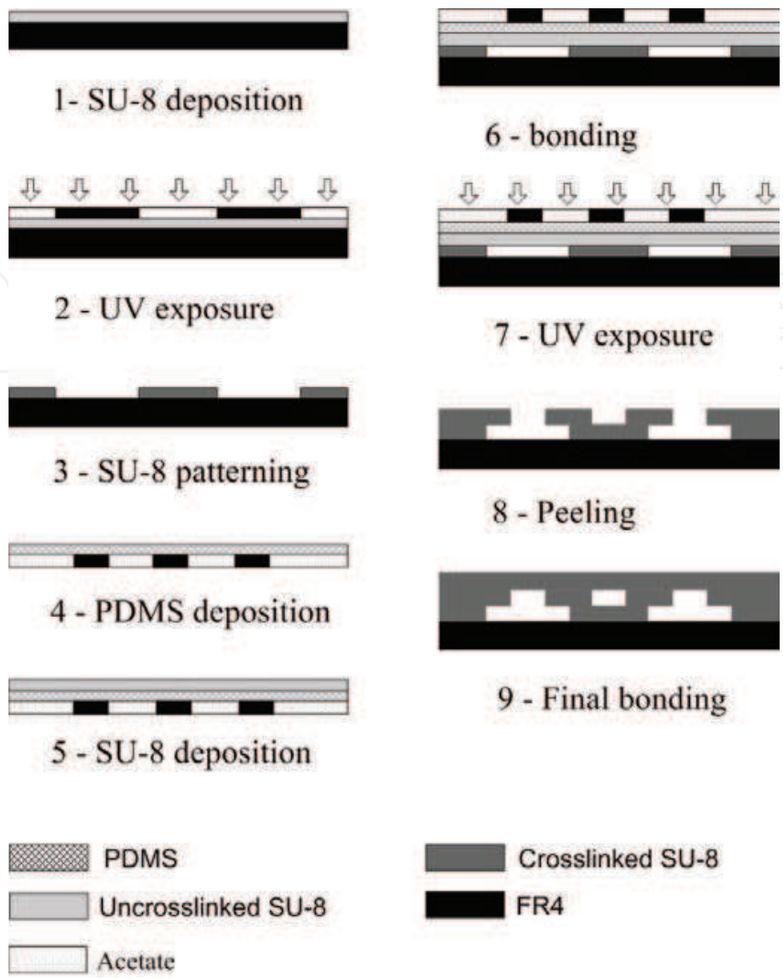


Fig. 9. Flow of fabrication process of a transferring process named BETTS.

Peristaltic micropumps have been widely used for LOC fluid flow generation, allowing the transport of a controlled fluid volume in clinical diagnosis and drug delivery applications Koch et al. (2009). Nevertheless, this alternative presents some disadvantages such as the large area required in the LOC device and the high power consumption to impulse the fluid. The solution presented in this chapter to minimize these limitations is the use of disposable microfluidic devices, based on a single use thermo-mechanical microvalve activation which releases a stored pressure to achieve a controlled fluid flow impulsion. This system can be easily integrated in a small area of the LOC, providing a portable reservoir of pneumatic energy.

The mechanism of differential pressure is a well known method in microfluidic fluid flow impulsion, where the use of epoxy resins such as SU-8 opens up new possibilities for the implementation of pressure-driven flow on-chip. Although polymers are typically several orders of magnitude more permeable to gas leakages than glass or metals, epoxy resins are characterized by a low gas permeability and thus can be used for simple and low-cost sealing of packages Murillo et al. (2010). In addition to this, SU-8 epoxy shows a decrease in gas permeability when the level of crosslinking is increased, being a suitable and interesting alternative for pressurized or vacuum microchambers fabrication Metz et al. (2004).

In this section two portable pressure driven flow devices for LOC applications are presented: vacuum and pressurized chambers.
The pressurized system consists in a monolithical SU-8 structure composed by a sealed microchamber connected to a valve that will be introduced in section 3.2. The chamber structure is connected to a microfluidic channel to seal it at a fixed and controlled pressure by an extra UV isolation step compatible with the traditional SU-8 fabrication process. The pressurized portable system SU-8 layout is shown in Fig. 11. To seal the chamber and store a fluid at a fixed pressure, low-viscous SU-8 is externally injected in the chamber hole through the control serpentine microchannel by means of a compressed air supply connected to a pressure transducer. The viscosity of the SU-8 supplied by Microchem is determined by the manufacturer by means of a code number (2005, 2025, 2150, etc.), where the lower number means lower SU-8 viscosity. Thus, to seal the chamber SU-8 2005 is employed. The dimensions of the microchannel are previously calculated according to the isothermal process for an ideal gas and the Boyle's law:

$$PV = k \rightarrow P_1 V_1 = P_2 V_2, \tag{1}$$

Where P_1 is the desired final pressure in the microchamber, V_1 is its volume, P_2 is the initial pressure before sealing process (atmospheric pressure), $V2$ the total air volume inside the structure and k is a constant. When the SU-8 2005 is injected through the inlet, the air volume entrapped inside the control channel at atmospheric pressure pushes the air in the chamber, proportionally increasing its pressure depending on the expression (1). As an example, the control microchannel area in the layout is calculated to be the same than the chamber area, in order to obtain 2 bar absolute pressure inside the chamber. Then, an UV exposure step polymerizes the liquid SU-8 inside the control channel to seal hermetically the chamber which is pressurized and ready for use. The stored pneumatic energy of the gas inside the chamber is expressed as follows, Hong et al. (2007).

$$E = \int P dV = P_1 V_1 ln \left(\frac{P_1}{P_F} \right) \tag{2}$$

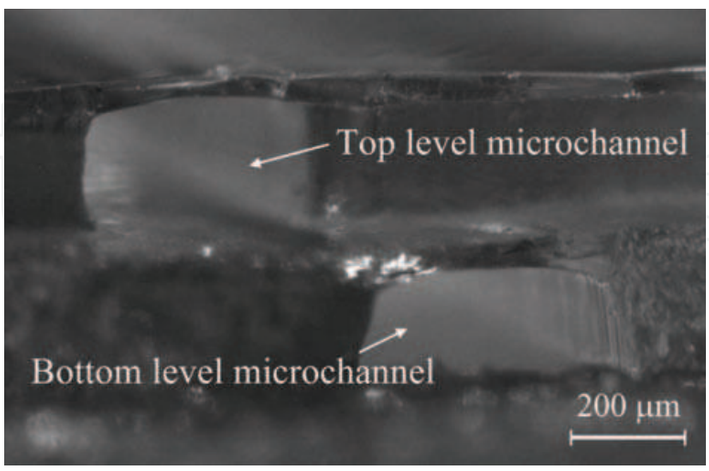


Fig. 10. Fabrication of three dimensional micro-channels network using BETTS process. The height of the walls is 200 μm while the thickness of the transferred layer is 40 μm. The width of the microchannels are 400 μm.



Fig. 11. Layout SU-8 mask for a pressurized chamber.

where P_1 is the absolute pressure of the gas in the chamber, V_1 is the volume of the gas in the chamber and P_F is the final pressure after the opening process (normally, it will be ambient pressure). This stored energy will be used to pump the working fluids in LOCs.

3.1.1 Fabrication of a pressurized chamber

The device implementation is simple to be carried out employing a traditional SU-8 fabrication process and PCB-based technology already explained in section 2. The first step is the consideration of a suitable and inexpensive substrate for the structure, where FR4 is chosen. A SU-8 2150 layer is deposited over the substrate by a spin coater and then soft baked for 15 min at 65°C and 90 min at 95°C. The result is a planar 200 μm thickness layer over the FR4, ready for a UV exposure step to transfer the structure shown in the layout of Fig. 11 in the SU-8. After a PEB step for 5 min at 65°C and 10 min at 95°C which polymerizes the SU-8, the board is immersed in SU-8 developer for 5 min and the final device structure patterned. Then, the board is carefully rinsed in isopropyl alcohol (IPA).

After this, the cover bonding process is carried out to close hermetically the structure by BETTS: A thin PDMS layer is spin coated over a transparent acetate film, cured by temperature and then a 40 μm thickness SU-8 2025 layer is deposited over the PDMS. This thin SU-8 layer is transferred placing the acetate film over the structure and exposing it to UV light during 2 min. This step produces a strong crosslinking between the SU-8 device structure and the SU-8 of the acetate, sealing completely the patterned layout. Then, the acetate with the PDMS is easily removed due to the low adhesion between the crosslinked SU-8 of the cover and the PDMS.

Once the SU-8 microchamber and control channel is finished and sealed by BETTS, a thin orifice is performed over the beginning of the microchannel in order to create the SU-8 2005 inlet. This fluid port is externally connected to a syringe pump than impulses the liquid SU-8 2005 through the microchannel and gradually increases the pressure of the air entrapped inside the chamber. The syringe flow rate is selected to pump 1 mL/min and the microchannel shape of a serpentine provides an easy method to precisely control the pumping time in order not to fill the chamber. With this method, the syringe is stopped when the SU-2005 reached the end of the channel before entering into the chamber, which would produce an undesired increment on its pressure. The SU-8 2005 is chosen as the pumping liquid due to its low viscosity, making easier the flow from the syringe through the control microchannel.

Then, with the syringe pump fixed and the microchannel filled with SU-8, the board is exposed to UV light for 5 min in controlled steps of 1 min in order to avoid an increment of the chamber temperature which would produce a pressure increment as well due to the ideal gas law. After the UV exposure step, the device is soft baked for 10 min at 95°C, achieving a strong crosslinking between the injected SU-8 and the microchannel SU-8 walls. Finally, the

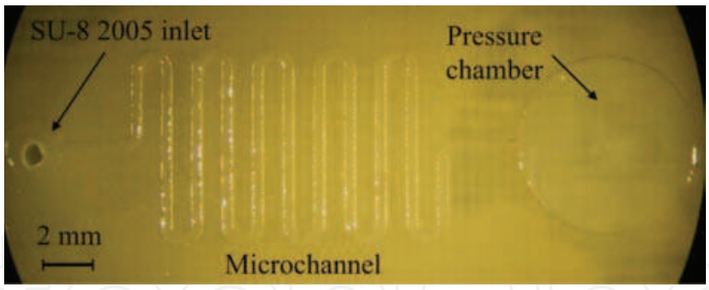


Fig. 12. Photograph of the pneumatic impulsion device.

syringe pump is disconnected from the device, and a 2 bar pressurized chamber hermetically sealed is obtained. The fabricated pneumatic impulsion device is show in Fig. 12. The total dimensions of the device are 10x35x1,75 mm^3, with a microchamber internal volume of 11 μL. Following this fabrication process, the manufacturing of a multiple array of pneumatic microdevices is easy to be carried out with the SU-8 layout mask shown in Fig. 13. The SU-8 2005 is distributed from a common inlet through the different microchannels in order to set a fixed pressure on each chamber. The dimensions of the distribution microchannels shown in the figure are calculated to push an identical volume of air into the chambers, in order to fabricate eight independent pressurized reservoirs fixed at the same pressure value. Moreover, it is easy to design the system with different stored pneumatic energies on each chamber just by changing the dimensions for every distribution channel. The white parts inside the microchambers shown in Fig. 13 are designed to work as pillars for the SU-8 chamber structure, supporting the cover fixed to the SU-8 walls during pressurizing step in order to avoid leakages or device breakages.

With the multiple structure presented, a microvalve could be easily added on each pressure chambers just by adding few fabrication steps in the manufacturing process, as is described in 5, developing a multi-pneumatic flow generator device capable of supplying eight different and independent fluid impulsions. From this point, the next step is to minimize the layout area of each device in order to copy the structure and to develop an array platform with tens of disposable pressurized chambers for complex LOC microfluidic systems.

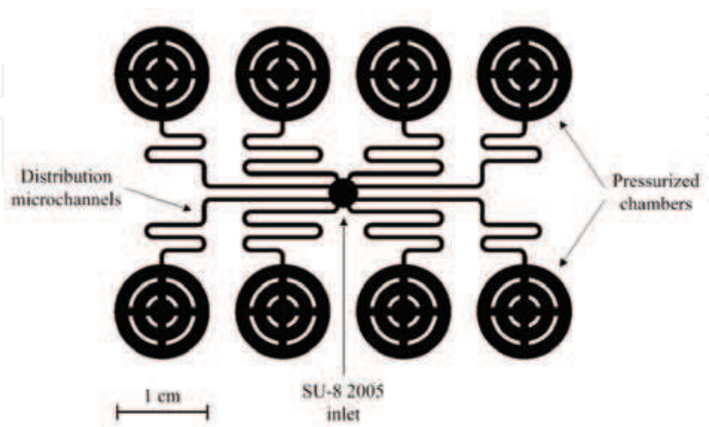


Fig. 13. Layout SU-8 mask of a multiple pressurized portable device

3.1.2 Fabrication of a vacuum chamber

Once the method and fabrication process for pressurizing SU-8 microstructures has been described, the manufacturing steps to develop vacuum chambers is explained as follows. In this case, the device layout just consists of the vacuum chamber without the need of using the control microchannel. The chamber dimensions are selected in order to calculate the volume of air displaced into the chamber when an activation is performed, according to ideal gas law equation (1). The initial fabrication steps to create the SU-8 microchamber are identical to the explained before with the pressurized system until cover layer is bonded to the structure. Now, a small orifice is drilled in the chamber in order to provide an air outlet for vacuum process. The FR4 board with the microchamber is placed inside a macro-vacuum chamber in the laboratory, which contains a syringe dispenser manually controlled from the outside. The SU-8 microchamber is then carefully placed underneath the dispenser, which is filled with SU-8 2025.

Then, the macro-vacuum chamber is sealed and starts to pump out the air contained inside the microchamber until a pressure of 0.1 bar is reached and observed by a pressure transducer externally connected to the vacuum pump. At this point, the dispenser is activated, releasing a droplet of SU-8 2025 over the cover orifice of the microchamber. The SU-8 2025 formulation plays a fundamental role due to its medium viscosity, which completely covers the lid orifice without filling the microchamber inside. Once the droplet has slightly entered into the orifice, a UV lamp illuminates the device, crosslinking the SU-8 droplet with the SU-8 cover of the chamber and thus sealing completely the microchamber at vacuum pressure.

Pressurized and vacuum portable systems explained above represent two inexpensive, fast prototyping and easy to fabricate alternatives for fluid flow generation. Moreover, the working fluids pressurized in the chambers could be either gas or liquid due to the low gas permeability of the SU-8 used in the device fabrication. As it is shown in section 5, the integration of these systems with other basic microfluidic components described throughout the chapter will lead in a portable and small LOC for fast microfluidic handling.

3.2 3D impulsion devices

Respect to the propulsion of fluid there are two main methods for driving the flow of fluids in microchannels: pressure-driven and electrokinetic. In the first case the propulsion is due to a difference of pressure between the ends of the microchannels, while in the second one the movement of charged molecules is due to an electric field. Both methods are effective, but the pressure-driven can be used for a wider range of solvents, even the not electrically conductive ones. On the other hand, the pressure driven uses to include an external pump or vacuum source, making non autonomous its operation.

One strategy of design to solve this disadvantage is to integrate microdevices that produces the difference of pressure. Furthermore, the disposability of many applications sets the trend to integrate one-shot devices. A simple way to obtain the difference of pressure is to open a chamber with an internal overpressure. With this approach there is no need of external impulsion so the connections and the complexity of the setup of the system is reduced. As example of this kind of devices, an autonomous microdevice for the impulsion in microfluidic applications is explained in detail in Aracil, Quero, Luque, Moreno & Perdigones (2010). The one-shot pneumatic impulsion device (OPID) is composed by a chamber and a single-use microvalve that connects its output port to the external microfluidic circuit where the fluid is propelled, Fig. 14. Due to the in-plane structure, a high integration with microfluidic and electronic components can be achieved. The activation is based in the combination of

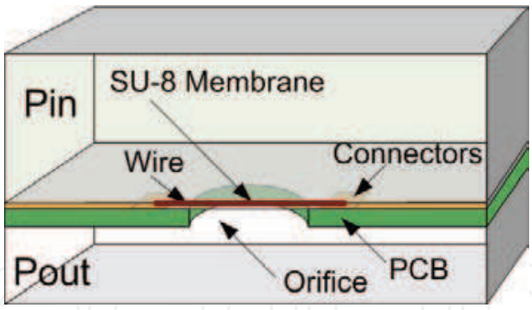


Fig. 14. Cross section of the 3D pneumatic impulsion device.

mechanical to thermal phenomena. The thermal effect is produced by making an electrical current flow through a resistor, implemented by a wire bonded gold filament, and the mechanical one by a differential pressure stored in the chamber. The combination of these phenomena at the time of activation produces a reduction of the required electrical energy with respect to other devices. The impulsion can be produced in the two directions, making a positive or negative difference pressure respect to external pressure. The fabrication of an array of devices can be easily implemented allowing the propulsion of fluid sequentially and in different directions. The device working can be seen in Fig. 15. These photos show three consecutive moments on the activation of the microdevice. Firstly, in (a), the microdevice is on repose. In (b), the current is applied, and changes on the membrane can be seen by the light changes. Finally, (c) shows the fluid coming into the chamber.

3.3 2D impulsion devices

An alternative to the 3D impulsion devices has been developed, consisting in a planar structure with the membrane acting as a vertical wall between the pressurized chamber and a microchannel Moreno & Quero (2010). The hybrid thermo-mechanical operating principle is similar: a gold microwire acting as a resistor crosses the SU-8 membrane that withstands the pressure difference between both sides. When an electric current is supplied to the wire the membrane heats up, drastically decreasing its fracture strength and causing the valve activation. The schematic of the 2D impulsion device design is shown in Fig. 16 and Fig. 17:
According to the mathematical approximation reported by Roark et al. (2001), the maximum bending stress σ_{max}, generated by a uniform pressure P on a clamped rectangular plate with a height Ly, a length Lx and a thickness h can be expressed as:

$$\sigma_{max} = cP\left(\frac{L_y}{h}\right)^2, \tag{3}$$

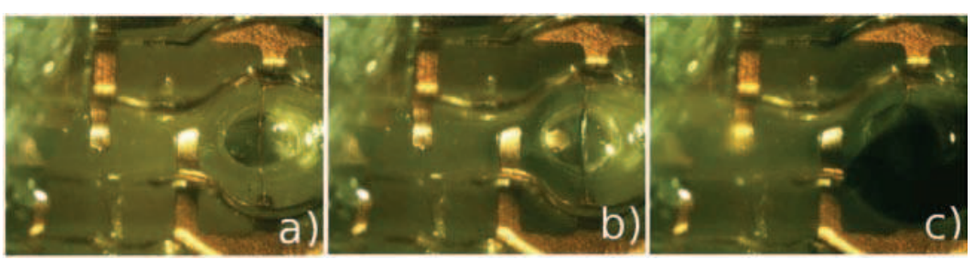


Fig. 15. Sequence of different frames of the device activation.



Fig. 16. Cross-section view of the 2D micro impulsion device. Pressure in the chamber is regulated through a PCB orifice.

where c is calculated by the polynomial least-squares curve fitting as a function of Ly and Lx. It is interesting to highlight that σ_{max} is thickness-to-width aspect ratio quadratic dependent, establishing the membrane aspect ratio and the pressure applied as main parameters involved in mechanical actuation. This fact determines that membrane fabrication is a critical step in the microvalve fabrication process.

The implementation of the microvalve employs SU-8 and PCB, integrating microfluidics with classical PCB electronic connections in a common substrate. The fabrication process starts with a photolithography and wet etching step of the copper layer on top of PCB, obtaining the connections to bond the gold wire. A flat bonding and a high accuracy in the gold microwire alignment are crucial tasks in order to heat the membrane on its mechanical weakest point, which is in the bottom center surface on the substrateMoreno et al. (2008). The next step is the deposition of a thick SU-8 layer over the board, making a softbake stage, a UV exposure, a post exposure bake and finally developing the SU-8 to pattern the final structure of the valve. Membranes with widths near to 45 μm and aspect ratios of 11 are achieved with nearly perfect vertical profiles. Two orifices are drilled on the PCB in the pressure chamber and in the right end of the microchannel to connect an external pump with the working pressure and to provide an inlet or outlet for the fluid flow, depending on the valve operation mode. Pressure on chamber will determine the fluid flow direction, establishing a reversible device operation bearing in mind that the microchannel is opened to outside air and consequently set at atmospheric pressure. If chamber pressure is higher than atmospheric, the device will operate as a microinjector, whereas with lower pressure than atmospheric the valve will work in microextractor mode, forcing the fluid contained in the inlet/outlet port through the channel towards the chamber.

Finally, the SU-8 cover is bonded to the structure by BETTS, sealing the chamber to avoid pressure leakages. The total dimensions of the device re 4x12x5 mm^3, with a microchannel length of 8 mm and a square section of 500x500 μm^2. A photograph of the microvalve is illustrated in Fig. 18:

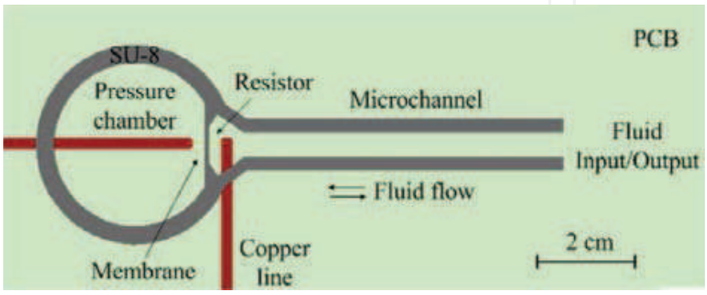


Fig. 17. Layout of the 2D micro impulsion device.

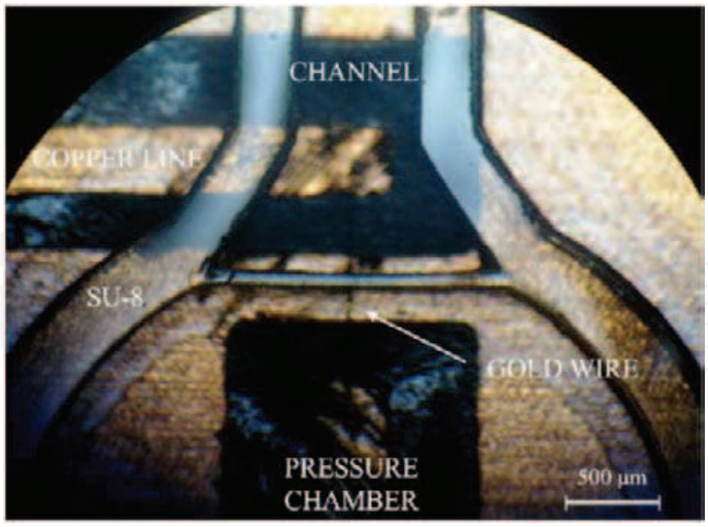


Fig. 18. Photograph of the SU-8 membrane crossed by the gold wire.

4. Flow regulation

4.1 Introduction

The control of fluids is an important issue when considering LOC devices and their applicability in biotechnology as is commented in section 1. Regarding microdevices to control or regulate the flow rates, there are many of them Oh & Ahn (2006) with different actuations. Among these devices, the most interesting ones are those which actuation is pneumatic due to the damage can be avoided in biological flows when through the devices. On this respect, there are many devices, for instance, the microvalves reported by Takao & Ishida (2003); Baek et al. (2005), all of them present negative gain, G, defined as

$$G = \left.\frac{\partial Q}{\partial P_1}\right|_{P_2} \leq 0, \tag{4}$$

where Q is the working flow rate, P_1 and P_2 are the control and working pressure, respectively.

4.2 Positive gain device

A recent publication Perdigones, Luque & Quero (2010a) demonstrates how the positive gain can be achieved. Thanks to the positive gain device a pneumatic microvalve can be fabricated. A simple cross section sketch of the microvalve is depicted in Fig. 19, which includes a control and a working channel. In the control channel is included the positive gain device, which is composed by two circular membranes with different diameters and a column linking them.
When positive pressure is applied in the control channel, the difference of membrane areas makes possible the aperture of the working channel, decreasing the fluidic resistance and increasing the flow rate. The behavior depends on the membrane and column diameters as is explained in Perdigones, Luque & Quero (2010a). If low Young modulus materials are used, i.e., PDMS, the shape of the large membrane must be chosen to be pseudo-elliptical Perdigones et al. (In press).
These kind of devices has been fabricated using the SU-8 technology in a FR4 substrate and using a combination of typical SU-8 process and BETTS (Fig. 20). On the other hand, the PDMS device has also been fabricated using the bonding technique commented above, Fig. 21 which

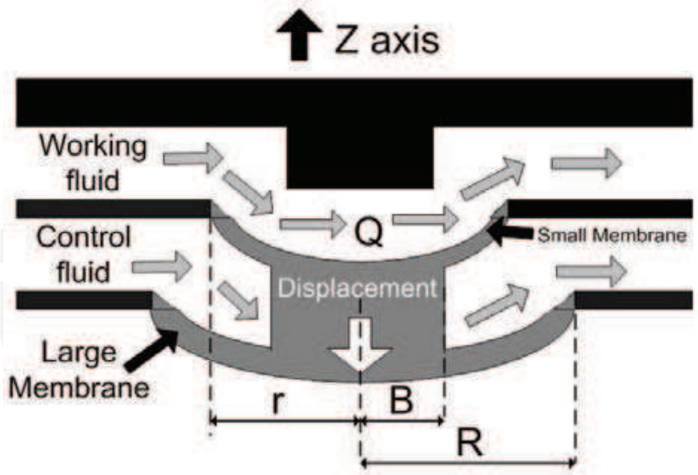


Fig. 19. Cross section of microvalve

section is Fig. 6 , in this case the device has pseudo-elliptical shape for the large membrane, unlike SU-8 device which membrane has circular shape.
The graphic which relates the working flow rate and the control pressure demonstrates the positive gain behavior. The slope of these curves is the gain of the microdevice, Perdigones, Luque & Quero (2010a). This slope is positive so the behavior of the device is governed by the positive gain, mathematically,

$$G = \left.\frac{\partial Q}{\partial P_1}\right|_{P_2} \geq 0, \tag{5}$$

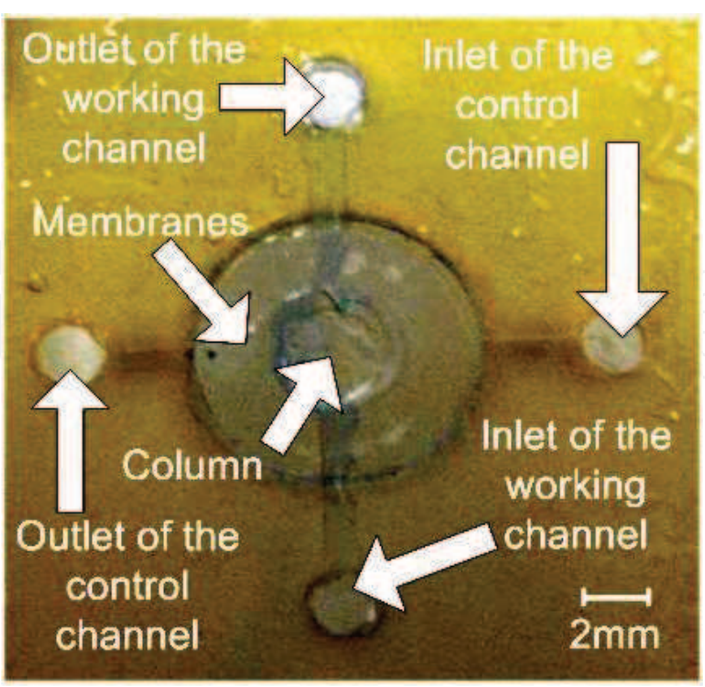


Fig. 20. Positive gain flow regulator fabricated using SU-8.

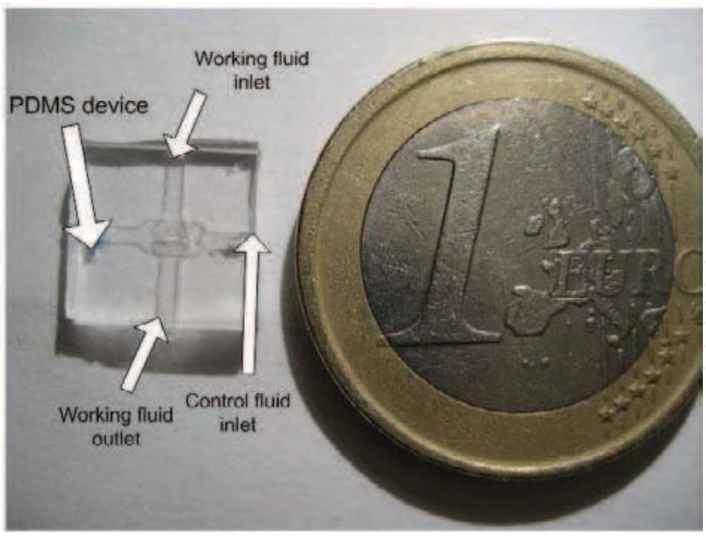


Fig. 21. Positive gain flow regulator fabricated using PDMS.

where Q is the working flow rate, P_1 and P_2 are the control and working pressure, respectively. The positive gain behavior provides improvement to the fluidic circuits, e.g., all pneumatic microvalves (positive and negative gain) can be controlled using positive pressure sources leaving out the vacuum systems. In addition, if a negative pressure is applied to the control channel, the microdevice is converted to a normally open microvalve because the control channel closes when that negative pressure is applied.

5. Integration

The final aim of this chapter is the integration of the previous components to achieve more complex devices. Therefore, an fundamental objective is to find compatible materials and fabrication processes in order to develop a monolithic, functional and autonomous fluidic microdevice without many manufacturing steps. In this task we will principally focus on SU-8 polymer and Printed Circuit Board (PCB) technology, taking advantage of the possibilities that these materials offer. A combination of the fabrication techniques commented before, such as BETTS, and new devices, such as pneumatic fluid impulsion devices, is essential to achieve this purpose. To illustrate this, next are detailed the design and fabrication steps involved in the fabrication of a portable microfluidic platform capable of storing, injecting, mixing and heating a chemical reagent and a human blood sample to finally analyze its glucose concentration.

The proposed design consists in a pressurized chamber connected to a single use microvalve in charge of driving the fluid flow through a microfluidic circuit. When the valve is activated, the pressure in the chamber pushes the fluid stored in two independent reservoirs, flowing towards a serpentine micromixer to finally reach a detection chamber where the mixture is heated and finally analyzed photometrically. A chemical reagent which contains enzyme glucose-oxidase is stored in one microreservoir, whereas a solution with a given glucose concentration is placed in the other reservoir. Both are connected by a microchannel to the entrance of a serpentine that mixes both fluids to finally reach the detection chamber, where the reaction takes place accelerated by the temperature supplied by the microheater. The chemical reaction results in a colored solution that can be measured in terms of optical

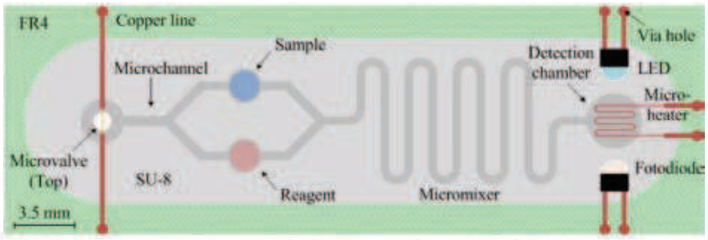


Fig. 22. Top layer of the microfluidic platform design, describing a potential integration of an optical sensor and heater.

absorbance by means of a light emitting diode and a photodetector. The commented design, developed in a two layer structure is illustrated in Fig. 22 and Fig. 23.
An interesting theoretic modeling for a pressure driven microfluidic design is the assumption of equivalent circuit theory (EC) in the context of microfluidics Bruus (2001). It derives its name from the 1:1 mathematical similarity between microfluidic components and the equivalent electronic components, with the basic assumption that the flow is incompressible and pressure driven with $Re < 1$. These low order models result very effective in describing the observed fluid dynamic effects and in addition have very attractive mathematical properties and highly intuitive applicability. The table 1 summarizes the equivalent circuit elements for microfluidic and electric circuits Vedel (2009).

Fluidic circuits	Electric circuits
Pressure drop = ΔP	Voltage = ΔV
Resistance = R_{hyd}	Resistance = R_{el}
Compliance = C_{hyd}	Capacitance = C_{el}
Inertance = L_{hyd}	Inductance = L_{el}

Table 1. Summary of equivalent circuit elements for microfluidic and electric circuits

With this method is possible to design the microchambers and microchannels dimensions of the microfluidic device in order to assure to entry of the mixed fluids in the detection chamber, avoiding the need of using complex fluid mechanics simulation software. Following the table above, the microchannels where replaced by fluidic resistances, R_{hyd}, comparing the linear relationship between an applied constant pressure difference ΔP and the resultant flow rate Q with the Ohm's law which describes the drop in electrical potential, ΔV across a resistor with resistance R in which a current I is running:

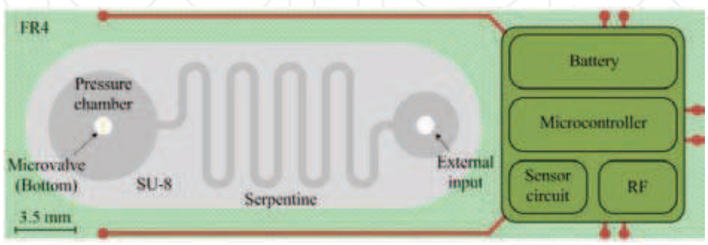


Fig. 23. Bottom layer of the microfluidic platform design, describing a potential integration of an electronic system.

$$\Delta P = \frac{128\mu L}{\pi D_H^4} Q = R_{hyd} Q \Longleftrightarrow \Delta V = RI \tag{6}$$

where μ is the fluid viscosity, L is the length of the microchannel and D_H the hydraulic diameter. In common microfabrication technology the microchannels are normally rectangular or square shaped, being necessary to add a relation between the microchannel height and width with the equivalent hydraulic diameter.

$$D_H = \frac{4S}{P_{wet}} = \frac{2wh}{w+h} \tag{7}$$

where S is the microchannel cross sectional area, P_{wet} is the wetted perimeter, w is the microchannel width and h is the microchannel height. According to the similarities shown between electric and fluidic principles, hydraulic compliance can be thought as a storage of volume in the hydraulic circuit since change in pressure will cause a change in volume, just as capacitance is a storage of electric charge. In this manner, the solution for the gas pressure $P(t)$ trapped in a chamber when it opens is easily seen to be analogous to the voltage across a discharging capacitor with a characteristic RC time. Moreover, if fluid flow branches off (e.g. in a T-junction) the total flow rate leaving and entering the junction must be identical because of the assumption of incompressible flow and mass conservation equation. These simple arguments illustrate the EC framework: understanding a microfluidic system as a network of parameters. The two arguments for series and parallel coupling are identical to Kirchhoff's laws from electric circuits, so electric network analysis is applied to EC models of microfluidics. With this method, the microfluidic device presented in this section can be designed and analyzed as a network of interconnected elements, as is shown in Fig. 24.

Once the device is theoretically studied and characterized, the next step is the fabrication process based on the integration of the different microdevices and fabrication techniques presented in previous sections.

The device is fabricated over a two-layer common PCB substrate, with the pneumatic impulsion system on the bottom layer connected through the microvalve to the top layer where the reagent and sample reservoirs with the microfluidic circuitry and detection chamber are placed. A photograph of the top and bottom SU-8 structures are shown in Fig. 25. A microhole is performed on top of the detection chamber to avoid air entrapment during device activation, as well as on the top of the pressure chamber to be used as an inlet for the air injection. To seal a fixed pressure in the chamber, low-viscous SU-8 2005 is externally injected in the chamber hole through the serpentine by means of a compressed air supply connected to a pressure transducer. When the desired pressure is reached in the chamber, the system is exposed to UV light in order to polymerize the liquid SU-8 entrapped inside the microchannel, closing hermetically the chamber. Finally, the sample and reagent fluids are injected and sealed inside the top layer reservoirs.

The microfluidic circuitry of the device has been successfully tested in the laboratory, achieving a controlled filling of the detection chamber. When an electric current is supplied to the gold wire embedded in the membrane, the pressure contained inside the chamber accelerates the valve activation, bringing the impulsion of the air and thus the fluid contained in the reservoirs almost instantly. The sample and reagent (e.g. glucose with its respective reagent) flows through the microchannel to the mixer, taking place the chemical reaction that makes the mixture to change its colour intensity, which is linearly proportional to the glucose concentration. When the colored mixture reaches the detection chamber and is heated up by

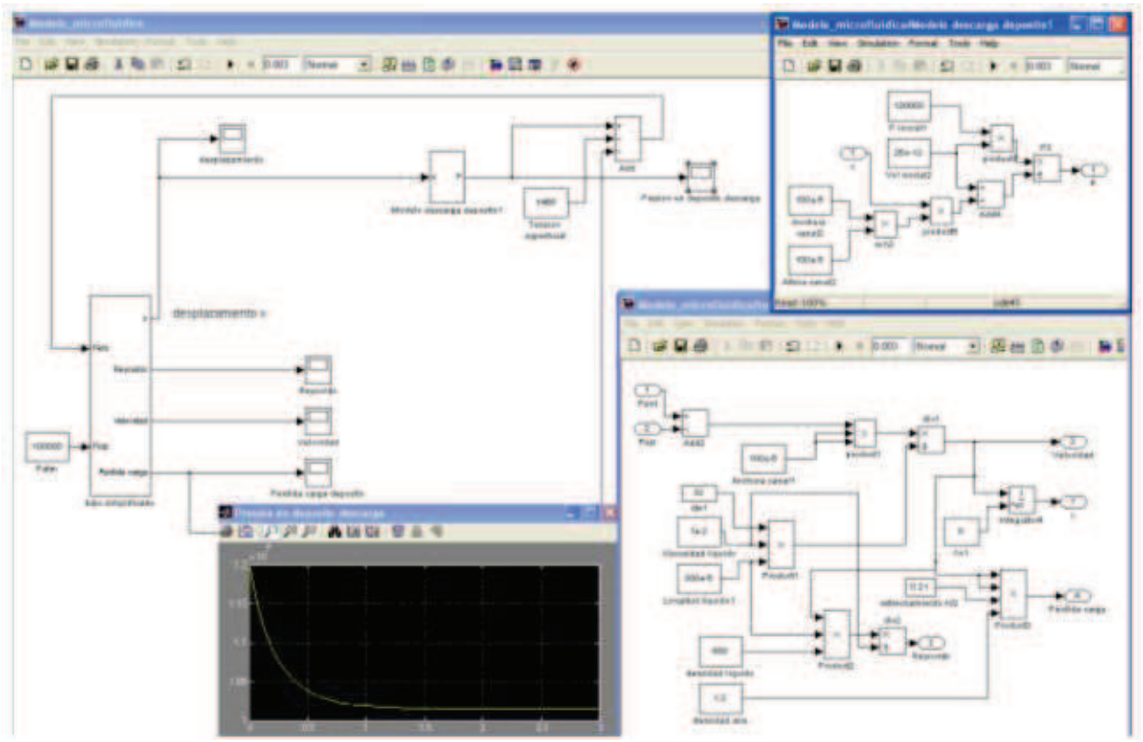


Fig. 24. Design of the microfluidic network using Matlab (Simulink)

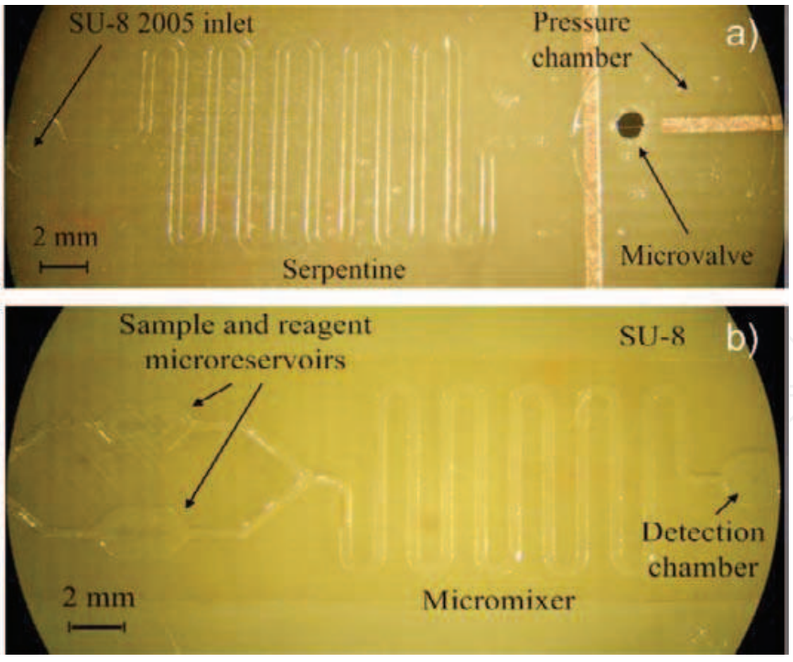


Fig. 25. Bottom and top layers, a) and b) respectively, of the SU-8 microfluidic platform, composed by the sample and reagent microreservoirs, the micromixer and the detection chamber.

the copper microlines, the photodiode will receive the light emitted by the LED through the detection chamber, generating a measurable electric current proportional to the intensity of the light.

6. Summary

This chapter has summarized design concepts, manufacturing processes and integration of MEMS devices for the realization of complex microfluidic systems. These implementations are based on polymer technology that enables the low cost and rapid prototyping of biomedical applications. The initial introduction has described the overall objectives and includes a comparison between the standard silicon MEMS technology and the polymeric one, remarking the facility of use and low cost of the latter. A review of standard processes using the most common materials, PDMS and SU-8, has been described in detail in section 2. The basic steps include deposition, photolithography, baking, and development. The machinery needed for the described processes are a photoplotter to print acetate masks, a spin-coater, a photolithography machine with mask aligner, a hot-plate and a chemical bank for polymer development. This machinery is available to the scientific community at a very reasonable cost compared to the significantly more expensive silicon technologies. Based on the previous basic manufacturing processes, a set of microfluidic devices have been introduced. A one-shot pneumatic impulsion device has been studied in section 3 due to its relevance in microfluidic systems, because it avoids the use of external pumps and complex microfluidic interfaces. Other devices, such as valves and flow regulators are also described in section 5. All these devices make use of a PCB as substrate to facilitate its integration with complementary electronic circuitry. These devices, together with many other that are found in literature, can be integrated to perform more complex microfluidic systems. Modeling a new fluidic design by means of the EC theory and simple simulation software allows the fast design of autonomous pneumatic microfluidic systems, also providing an easy design tool for a wide variety of pressure driven LOC devices, considerably reducing the prototyping and development time. An example of a microfluidic system modeling has been developed in section 5. Finally, an example of a basic LOC including an impulsion device, a mixer and a reaction chamber has been fabricated. The final device requires 0.35J of electrical energy supplied to activate the impulsion device, with a pressure of 3 bar stored in the chamber in order to assure the complete filling of the detection chamber by the fluid to be analyzed. The total time to implement such a system is only one day, thus facilitating a fast improvement of the designs. This example can be easily generalized to implement much more complex microfluidic systems.

7. References

Abgrall, P., Charlot, S., Fulcrand, R., Paul, L., Boukabache, A. & Gue, A. (2008). Low-stress fabrication of 3d polymer free standing structures using lamination of photosensitive films, *Microsyst. Technol.* 14(8): 1205–1214.

Aracil, C., Perdigones, F., Moreno, J. M. & Quero, J. M. (2010). BETTS: bonding, exposing and transferring technique in SU-8 for microsystems fabrication, *Journal of Micromechanics and Microengineering* 20: 035088.

Aracil, C., Quero, J. M., Luque, A., Moreno, J. M. & Perdigones, F. (2010). Pneumatic impulsion device for microfluidic systems, *Sensors and Actuators A: Physical* vol. 163, issue 1: pp. 247–254.

Baek, J. Y., Park, J. Y., Ju, J. I., Lee, T. S. & Lee, S. H. (2005). A pneumatically controllable flexible and polymeric microfluidic valve fabricated via in situ development, *Journal of Micromechanics and Microengineering* 15(5): 1015.

Bruus, H. (2001). *Theoretical Microfluidics*, McGraw-Hill.

Chuang, Y.-J., Tseng, F.-G., Cheng, J.-H. & Lin, W.-K. (2003). A novel fabrication method of embedded micro-channels by using SU-8 thick-film photoresists, *Sens. Actuators A, Phys.* 103(1-2): 64 – 69.

Chung, C. & Allen, M. (2005). Uncrosslinked SU-8 as a sacrificial material, *J. Micromech. Microeng.* 15(1): 113–121.

Dean, R. N. & Luque, A. (2009). Applications of microelectromechanical systems in industrial processes and services, 56: 913–925.

Duffy, D., McDonald, J. C., Schueller, O. & Whitesides, G. M. (1998). Rapid prototyping of microfluidic systems in poly(dimethylsiloxane), *Anal. Chem.* 70(23): 4974 – 4984.

Eddings, M. A., Johnson, M. A. & Gale, B. K. (2008). Determining the optimal PDMS PDMS bonding technique for microfluidic devices, *Journal of Micromechanics and Microengineering* 18: 067001.

Ezkerra, A., Fernandez, L. J., Mayora, K. & Ruano-Lopez, J. M. (2007). Fabrication of SU-8 free-standing structures embedded in microchannelsfor microfluidic control, *J. Micromech. Microeng.* 17(11): 2264–2271.

Guerin, L., Bossel, M., Demierre, M., Calmes, S. & Renaud, P. (1997). Simple and low cost fabrication of embedded micro-channels by using a new thick-film photoplastic, *TRANSDUCERS '97. International Conference on Solid State Sensors and Actuators, Chicago*, Vol. 2, pp. 1419–1422.

Haefliger, D. & Boisen, A. (2006). Three-dimensional microfabrication in negative resist using printed masks, *J. Micromech. Microeng.* 16(5): 951–957.

Henry, S., McAllister, D. V., Allen, M. G. & Prausnitz, M. R. (1998). Micromachined needles for the transdermal delivery of drugs, *Proceedings of the IEEE Eleventh Annual International Workshop on Micro Electro Mechanical Systems, Heidelberg, Germany*, pp. 494–498.

Hong, C. C., Choi, J. W. & Ahn, C. H. (2007). An on-chip air-bursting detonator for driving fluids on disposable lab-on-a-chip systems, *Journal of Micromechanics and Microengineering* 17: 410–417.

Huang, H. & Fu, C. (2007). Different fabrication methods of out-of-plane polymer hollow needle arrays and their variations, *J. Micromech. Microeng.* 17: 393–402.

Koch, C., Remcho, V. & Ingle, J. (2009). Chemical,pdms and tubing-based peristaltic micropumps with direct actuation, *Sensors and Actuators B: Chemical* 135(2): 664–670.

Kovacs, G. T. A., Maluf, N. I. & Petersen, K. E. (1998). Bulk micromachining of silicon, 86(8): 1536–1551.

Laser, D. J. & Santiago, J. G. (2004). A review of micropumps, *Journal of Micromechanics and Microengineering* 14: R35–R64.

Lim, Y. C., Kouzani, A. Z., & Duan, W. (2010). Lab-on-a-chip: a component view, *Microsyst. Technol.* 16:1995-2015.

Lorenz, H., Despont, M., Fahrni, N., LaBianca, N., Renaud, P. & Vettiger, P. (1997). SU-8: a low-cost negative resist for MEMS, *Journal of Micromechanics and Microengineering* 7: 121–124.

Mata, A., Fleischman, A. J. & Roy, S. (2006). Fabrication of multi-layer su-8 microstructures, *Journal of Micromechanics and Microengineering* 16: 276–284.

McDonald, J. C. & Whitesides, G. M. (2002). Poly(dimethylsiloxane) as a material for fabricating microfluidic devices, *Accounts of Chemical Research* 35(7): 491 – 499.

Metz, S., Jiguet, S., Bertsch, A., & Renaud. (2004). Polyimide and SU-8 microfluidic devices manufactured by heat-depolymerizable sacrificial material technique, *Lab Chip* 4:114-120.

Moreno, J. M. & Quero, J. M. (2010). A novel single-use SU-8 microvalve for pressure-driven microfluidic applications, *Journal of Micromechanics and Microengineering* 20: 015005.

Moreno, M., Aracil, C. & Quero, J. (2008). High-integrated microvalve for lab-on-chip biomedical applications, pp. 313 –316.

Murillo, G.,Davis, Z. J., Keller, S., Abadal, G., Agusti, J., Cagliani, A., Noeth, N., Boisen, A. & Barniol, N. (2010). Novel SU-8 based vacuum wafer-level packaging for MEMS devices,*Microelectronic Engineering* 87:1173-1176.

Oh, K. W. & Ahn, C. H. (2006). A review of microvalves, *Journal of Micromechanics and Microengineering* 16: R13–R39.

Patel, J. N., Kaminska, B., Gray, B. L. & Gates, B. D. (2008). Pdms as a sacrificial substrate for SU-8-based biomedical and microfluidic applications, *J. Micromech. Microeng.* 18(9): 095028 (11pp).

Perdigones, F., Luque, A. & Quero, J. M. (2010a). Novel structure for a pneumatically controlled flow regulator with positive gain, *Journal of Microelectromechanical Systems.* 19(5): 1070 – 1078.

Perdigones, F., Luque, A. & Quero, J. M. (2010b). PDMS microdevice for precise liquid aspiration in the submicroliter range based on the Venturi effect, *Microelectronic Engineering* 87(11): 2103 – 2109.

Perdigones, F., Moreno, J. M., Luque, A. & Quero, J. M. (2010). Characterisation of the fabrication process of freestanding SU-8 microstructures integrated in printing circuit board in microelectromechanical systems, *Micro and Nano Letters* 5: 7–13.

Perdigones, F., Luque, A. & Quero, J. M. (In press). Highly integrable flow regulator with positive gain, *Journal of Microelectromechanical Systems* In press.

Petersen, K. E. (1982). Silicon as a mechanical material, 70(5): 420–457.

Roark, R. J., Budynas, R. G. & Young, W. C. (2001). *Roark's Formulas for stress and strain*, McGraw-Hill.

Status of the MEMS industry (2008). Yole Dveloppement.

Takao, H. & Ishida, M. (2003). Microfluidic integrated circuits for signal processing using analogous relationship between pneumatic microvalve and MOSFET, *Journal of Microelectromechanical Systems* 12(4): 497–505.

Vedel, S. (2009). *Millisecond dynamics in microfluidics: Equivalent circuit theory and experiment*, PhD thesis, DTU Nanotech, Department of Micro and Nanotechnology.



Biomedical Engineering, Trends in Electronics, Communications and Software

Edited by Mr Anthony Laskovski

ISBN 978-953-307-475-7
Hard cover, 736 pages
Publisher InTech
Published online 08, January, 2011
Published in print edition January, 2011

Rapid technological developments in the last century have brought the field of biomedical engineering into a totally new realm. Breakthroughs in materials science, imaging, electronics and, more recently, the information age have improved our understanding of the human body. As a result, the field of biomedical engineering is thriving, with innovations that aim to improve the quality and reduce the cost of medical care. This book is the first in a series of three that will present recent trends in biomedical engineering, with a particular focus on applications in electronics and communications. More specifically: wireless monitoring, sensors, medical imaging and the management of medical information are covered, among other subjects.

How to reference

In order to correctly reference this scholarly work, feel free to copy and paste the following:

Francisco Perdigones, Jose Miguel Moreno, Antonio Luque, Carmen Aracil and Jose Quero (2011). Microsystem Technologies for Biomedical Applications, Biomedical Engineering, Trends in Electronics, Communications and Software, Mr Anthony Laskovski (Ed.), ISBN: 978-953-307-475-7, InTech, Available from: http://www.intechopen.com/books/biomedical-engineering-trends-in-electronics-communications-and-software/microsystem-technologies-for-biomedical-applications

INTECH
open science | open minds

InTech Europe
University Campus STeP Ri
Slavka Krautzeka 83/A
51000 Rijeka, Croatia
Phone: +385 (51) 770 447
Fax: +385 (51) 686 166
www.intechopen.com

InTech China
Unit 405, Office Block, Hotel Equatorial Shanghai
No.65, Yan An Road (West), Shanghai, 200040, China
中国上海市延安西路65号上海国际贵都大饭店办公楼405单元
Phone: +86-21-62489820
Fax: +86-21-62489821

© 2011 The Author(s). Licensee IntechOpen. This chapter is distributed under the terms of the Creative Commons Attribution-NonCommercial-ShareAlike-3.0 License, which permits use, distribution and reproduction for non-commercial purposes, provided the original is properly cited and derivative works building on this content are distributed under the same license.

IntechOpen

IntechOpen